Journal of Membrane Science and Research 4 (2018) 146-157

Journal of Membrane Science & Research

journal homepage: www.msrjournal.com

Research Paper

Fabrication of Nanocomposite Membrane via Combined Electrospinning and Casting Technique for Direct Methanol Fuel Cell

H. Junoh [a], Juhana Jaafar [a,*], N.A.M. Nor [a], Nuha Awang [a], M.N.A.M. Norddin [a], A.F. Ismail [a], M.H.D. Othman [a], Mukhlis A. Rahman [a], F. Aziz [a], N. Yusof [a], W.N.W. Salleh [a], R. Naim [b]

[a] *Advanced Membrane Technology Research Centre (AMTEC), Universiti Teknologi Malaysia, 81310 UTM Skudai, Johor Bahru, Malaysia*
Faculty of Petroleum and Renewable Energy Engineering, Universiti Teknologi Malaysia, 81310 UTM Skudai, Johor Bahru, Malaysia
[b] *Faculty of Chemical and Natural Resources Engineering, Universiti Malaysia Pahang, Lebuhraya Tun Razak, 26300 Kuantan, Pahang, Malaysia*

Article info

Received 2017-07-26
Revised 2017-12-05
Accepted 2017-12-16
Available online 2017-12-16

Keywords

Electrospinning
Cloisite15A®
SPEEK
DMFC
Nanocomposite
Nanofibers

Graphical abstract

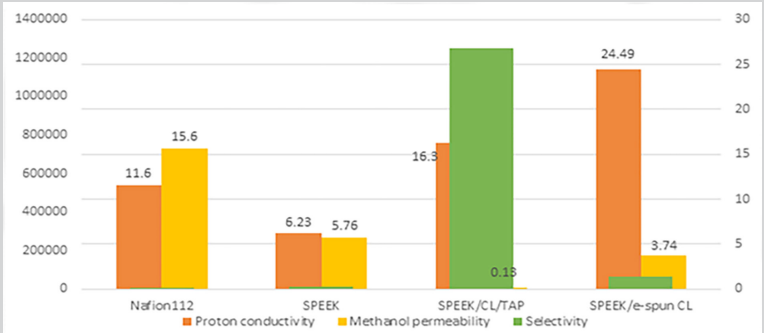

Highlights

- Cloisite 15A® was well electrospun with an average diameter of nanofiber of approximately 187.4 nm.
- Cloisite15A® particles at nanometer range were uniformly distributed and 66% smaller than in SPEEK63/2.5CL/5.0TAP.
- Dispersion state of Cloisite15A® fell into intercalated phase.
- A very small amount of Cloisite15A® (0.05wt.%) in SPEEK63/e-spun CL had successfully enhanced the proton conductivity up to 50%.

Abstract

Emergence of nanotechnology has resulted in the introduction of the electrospinning process in fabricating and characterising the polymer electrolyte membrane from the sulfonated poly (ether ether ketone) (SPEEK) nanocomposite membrane comprised of electrospun Cloisite15A® (e-spun CL) for direct methanol fuel cell (DMFC). Poly (ether ether ketone) polymer is sulfonated up to 63% by sulfuric acid. SPEEK63/e-spun CL nanofibers were fabricated via electrospinning in which SPEEK63 was used as carrier polymer while the SPEEK63/e-spun CL nanocomposite membrane was obtained by the casting method. Characterizations on physical, morphological and thermal properties of SPEEK63/e-spun CL were conducted and compared to the SPEEK membrane fabricated by casting simple mixing 2.5wt.% Cloisite15A® and 5.0wt.% triaminopyrimidine solution (SPEEK63/2.5CL/5.0TAP). Scanning electron microscopy (SEM) showed well electrospun Cloisite15A® with an average diameter nanofiber around 187.4 nm. Moreover, field emission scanning electron microscopy (FESEM) revealed that Cloisite15A® particles at a nanometer range were uniformly distributed and 66% smaller than those in SPEEK63/2.5CL/5.0TAP. Furthermore, x-ray diffraction proved that the dispersion state of Cloisite15A® fell into an intercalated phase. A very small amount of Cloisite15A® (0.05wt.%) in SPEEK63/e-spun CL successfully enhanced the proton conductivity up to 50%, whereas, unfortunately the methanol permeability value was 27 times higher than SPEEK63/2.5CL/5.0TAP. Proton conductivity and methanol permeability of SPEEK63/e-spun CL were 24.49 x 10^{-3} Scm^{-1} and 3.74 x 10^{-7} cms^{-1}, respectively. Even though this study contributed to 95% selectivity lower than SPEEK63/2.5CL/5.0TAP, electrospinning showed a promising technique to further reduce original sized Cloisite15A® particles from mixed size (μm and nm) to nanometer sized. In addition, by fine tuning, the dispersion of Cloisite15A® enhances the SPEEK63/e-spun CL performance in DMFC.

© 2018 MPRL. All rights reserved.

1. Introduction

Nowadays, the research and development of renewable energy have been increasing yearly. Among several well-known types of renewable energy are solar energy, wind energy, geothermal energy, bioenergy, hydropower and ocean energy. In addition, fuel cell has also been gaining attention for its promising alternative in providing energy sources. The research and development (R&D) on proton electrolyte membrane (PEM) is foreseen to

* Corresponding author at: Phone: +607-5535352; fax: +607-5535925
E-mail address: juhana@petroleum.utm.my (J. Jaafar)

DOI: 10.22079/JMSR.2017.68712.1149

generate more significant contributions compared to other parts in the fuel cell system. PEM is constantly expressed as the "nerve" or "heart" of a fuel cell system as it plays the most crucial task in allowing and repelling protons and electrons. Such characteristics determine the efficiency of fuel cells as a whole, concurrently providing a beneficial impact on environmental as well as economic views.

Layered silicates-polymer nanocomposite is a new polymer electrolyte membrane (PEM) that has recently attained a great deal of interest due to improvements on mechanical, thermal and barrier properties of the pure polymer [1]. Compared to the corresponding pure polymer as well as commercial Nafion® membranes, many polymer-inorganic nanocomposite membranes are shown to have lower fuel permeability, though they do share similar or improved proton conductivities due to nano-dispersion of layered silicates all over the polymer matrix [2].

A long list of advantages to base materials such as the flexibility and process ability of polymer, as well as the selectivity and thermal stability of the inorganic fillers are contributed from the aforementioned properties. By adding inorganic nanofillers, it may affect the membrane cell in two ways: 1) the uniform nanosized distribution of inorganic filler particles produces a winding diffusion pathway which can hinder the fuel from transferring into the nanocomposite membrane, and 2) the complete morphological structure allows more cations to be mobile and available for conduction [2]. Inorganic fillers have decreased the cluster size of the parent polymer, thus leading to a complete exfoliated morphology structure (referring to 2). These exfoliated structures would acquire the results mentioned by narrowing the size of both ion clusters and some well-distributed inorganic fillers in the nanocomposite membrane, simultaneously increasing proton conductivity of the referred membrane [3]. According to Jaafar et al. [4], the loading effect of inorganic filler also plays a role in determining the performance of proton conductivity. Moreover, the smaller the size of particles, the larger the surface area of dispersed nanosized particles in a polymer matrix, and therefore a decrease in the degree of crystallinity of polymer segments. In fact, this phenomenon contributes to the larger ionic mobility that eventually increased proton conduction [5, 6].

Electrospinning seems to be a good solution in generating nanosized particles, as well as altering the structure of the polymer-inorganic electrolyte membrane. This is due to electrospinning's nature – versatility. In fact, the process stated is deemed favourable in developing highly porous, patterned, nano-fibrous polymeric materials of nanofibers [7]. Other than that, there are other advantages to electrospinning, specifically its low cost, capability and high speed; making it a component with great potential in producing nanocomposite fibres [8]. Its unique properties such as being extremely long, having large surface area, complex pore size alignment on either woven or nonwoven fiber make it feasible to work with in various applications [9-12], especially for the polymer electrolyte membrane. It is no doubt that the combination of nanosized particles and the upsides of polymer electrolyte is a great help to focus on the nanocomposite polymer electrolyte membrane within the laboratory, as well as industrial applications.

Nafion®, a sulfonated tetrafluoroethylene developed by Walther Grot (DuPont), is an interesting and most commonly used material, utilised as a proton exchange membrane in PEM fuel cells [13]. Unfortunately, Nafion® molecules are difficult to be electrospun due to their insolubility property within solvents [13]. This is due to the formation of micelles, which somehow leads to the decrease of molecules within chain entanglement. When that happens, a high molecular weight carrier is needed to cater the problems faced by Nafion® [14]. Previously, Jaafar et al. [4] had successfully fabricated Cloisite15A® within the SPEEK matrix which is comparable to Nafion® [4]. However, their method is still limited due to the size distribution of Cloisite15A® particles. Therefore, in this study, by introducing the electrospinning process of SPEEK as the base polymer matrix, along with Cloisite15A® nanoclay as an inorganic filler, it is strongly believed that a novel polymer-nanocomposite electrolyte membrane with reduced filler size down to nanostructure can be successfully developed.

2. Experimental

2.1. Materials

Poly (ether ether ketone) (PEEK) polymer was obtained from Victrex US Inc. Ltd in powder form. Sulphuric acid (H_2SO_4) of 95% to 98% concentration was purchased from QRex and it was a strong sulfonation agent that has been used widely to test sulfonation reaction. However, DMAc was obtained from Sigma-Aldrich and used as supplier for a solvent to dissolve SPEEK. Cloisite15A®, a natural montmorillonite, though modified with quaternary ammonium salt, was acquired from Southern Clay Product. Table 1 and Table 2 below show the properties of PEEK and Cloisite15A®, respectively.

Table 1
Properties of PEEK.

Properties	Value
Molecular weight ($gmol^{-1}$)	39200
Glass transition temperature (°C)	143
Density (g/cm^3)	1.30
Melting temperature (**°C**)	343
Solvent resistance	Soluble in (H_2SO_4, CH_3SO_3H) Insoluble in (DMF, DMAc, NMP)

Table 2
Physical and chemical properties of Cloisite15A®.

Properties	Value
Physical state	Solid
Form	Powder
Color	Off-white
Odor	Odorless
Auto-ignition temperature (**°C**)	190 (thin film ignition)
Specific gravity	1.4-1.8

2.2. Formation of sulfonated poly (ether ether ketone) (SPEEK)

The experiment on sulfonation reaction was conducted at room temperature, with a mixture of poly (ether ether ketone) (PEEK) and sulfuric acid used as the sulfonation agent for PEEK. Initially, a mixture of 50 g PEEK and 1000 ml sulfuric acid was magnetically stirred at room temperature in sulfonation reactions for 1 hour. The solution was then continuously stirred for 3 hours at 55 °C [15]. The sulfonated polymer was then recovered by precipitating the acid polymer solution into a large excess of ice water. The resulted SPEEK polymer was filtered and washed thoroughly with deionized water until its pH became 6~7. Only then the sulfonated PEEK was left to dry in the drying oven at 80 °C for 24 hours, and then kept in it at 50 °C instead to maintain the humidity.

2.3. Electrospun nanocomposite fiber preparation through electrospinning

Within the preparation of the electrospun nanocomposite polymeric solution, dried SPEEK was dissolved in DMAc solution in order to prepare 20 wt.% of SPEEK solution. The desired amount of Cloisite15A® was then added to a small amount of DMAc in a separate container to prepare 0.05 wt.% Cloisite15A® solution (based on 1wt% of Cloisite15A® in 1mL of solvent). Both solutions were vigorously stirred for 24 h at room temperature. Finally, in one container, the final solution was stirred for another 24 h, still at room temperature to produce a homogeneous solution prior to the electrospinning process. 20wt% of SPEEK containing 0.05 wt.% Cloisite15A® was used as the electrospinning precursor solution. The dope solution was placed in a 10ml syringe with a metal needle of 0.34 mm in diameter. A power supply was also utilised to provide high voltage, which increased gradually from 0kV ~ 16 kV to the syringe needle tip until the jet became stable. Aluminium foil was used as the collector at a distance of 20 cm. A flow rate of 0.6 ml/hr was also applied on the dope solution, whereas throughout the electrospinning process, room temperature was maintained. Then, the electrospun fiber was collected as a fiber mat and left to dry for 12 hr to complete hydrolysis.

2.4. Preparation of nanocomposite membrane

As the electrospun nanofiber possesses low mechanical strength, a support membrane is needed to render the drawback of nanocomposite fiber SPEEK/Cloisite15A® to be applicable in the DMFC system. A neat SPEEK solution was also considered to provide support for the electrospun nanocomposite fiber. Consequently, dried SPEEK was then dissolved in DMAc solution to prepare 16wt% of SPEEK solution, which was then vigorously stirred for 24 h at room temperature, producing a homogeneous solution. The prepared electrospun SPEEK/Cloisite15A® nanocomposite fiber mat (1 gram) was then dipped into the support membrane solution (SPEEK 16 wt.%) and stirred for 24 hours, to generate a homogeneous solution. The

solution was then casted on a petri dish, allowing a thin film of nanocomposite membrane to form. It was then dried via oven for 24 hr at 80°C, and then one more at 100°C for 6 hr – to ensure that the residual solvent is completely removed. By immersing the petri dish into water, it allowed the membrane to be easily detached, which was then cured in the oven for 3 days at 80°C. At the end, the resultant membrane was treated with 1M sulphuric acid solution for 1 day at room temperature and subsequently rinsed with water several times to remove the remaining acid and assure that the sulfonated solution was in H form.

2.5. Nuclear magnetic resonance spectroscopy

Hydrogen-nuclear magnetic resonance (H^1NMR) spectroscopy was used to determine the degree of sulfonation (DS) of membranes via comparative integration of distinct aromatic signals according to the following equation:

$$\frac{n}{12-2n} = \frac{\Delta H_{13}}{\sum \Delta H_{(integrated\ signal)}} \quad (0 \leq n \leq 1) \tag{1}$$

where n is the number of H_{13} per repeat unit. ΔH_{13} is the area under the graph for the H_{13} region, equivalent to the sulfonic acid group content, and $\sum \Delta H_{(integrated\ signal)}$ is the total area under the graph for all the other aromatic hydrogen regions. The DS = n × 100%.

2.6. Membrane characterizations

The morphological structure and fiber diameter of the electrospun nanocomposite fibers were characterised by using scanning electron microscopy (SEM) (Hitachi, TM3000) with magnification up to 10,000-20,000. An energy dispersive X-ray spectrometer (EDX) using an acceleration voltage of 15kV and magnification of 5000x was employed for elemental analysis in order to confirm the appearance of Cloisite15A® nanoparticles within the electrospun nanocomposite fiber. The morphology of the SPEEK/e-spun Cloisite15A® nanocomposite membrane was investigated based on the field emission scanning electron microscopy (FESEM) (Hitachi SU8020) with magnification in the range of 10x to 300. 000x was also used and an energy dispersive X-ray spectrometer (EDX) with acceleration voltage of 15kV and magnification of 5000x was also used for elemental analysis in order to confirm the appearance of Cloisite15A® nanoparticles.

2.7. X-ray diffraction analysis (XRD)

The dispersion degree of Cloisite15A® was monitored using Bruker D8 Advance diffractometer with Dynamic Scintillation Detector of low background (0.4 cps) and high dynamic range (up to 2 x 10^6 cps). The system used a CuKα source (λ = 0.154060 nm) at 40 kV and 40 mA. Diffractogram, on the other hand, was scanned with a scanning rate of 2° min^{-1} within 2θ range of 2°-12° at room temperature. The d – spacing of Cloisite15A® in nanocomposites was also calculated with reference to Bragg's equation based on XRD results:

$$d = \frac{n\lambda}{2\sin\theta} \tag{2}$$

where d is the spacing n=1 in our calculation.

2.8. Physical properties of nanocomposite membranes

The physical properties of nanocomposite membranes were categorised based on water uptake, proton conductivity and methanol permeability. The selected membrane was then soaked in water at room temperature for as long as the membrane integrity could sustain. The water uptake was calculated as follows:

$$\text{water uptake} = \frac{W_{wet} - W_{dry}}{W_{dry}} \times 100\% \tag{3}$$

whereby, W_{wet} is the weight of the wet membrane and W_{dry} is the weight of the dry membrane.

The proton conductivity of the hydrated membrane was measured by using the AC impedance technique instead, whereby a Solartron 1260 impedance gain phase analyser, over a frequency range of 10 MHz – 10 Hz with 50 – 500 mV oscillating voltage. All impendent measurements were performed at room temperature with 100% humidity. The membrane resistance, R, was obtained from the intercept of the impedance curve with the real-axis at high frequency end. The proton conductivity of the membrane, σ (Scm^{-1}) was calculated accordingly:

$$\sigma = \frac{d}{RS} \tag{4}$$

in which, d and S refer to thickness of the hydrated membrane and the area of the membrane sample, respectively. Figure 1 illustrates the schematic diagram of proton conductivity cell.

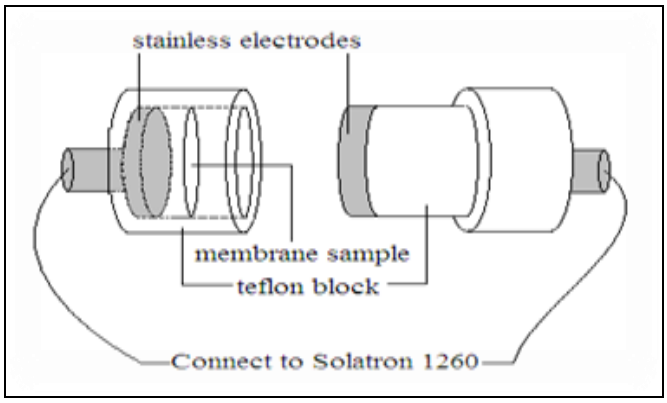

Fig. 1. Schematic diagram of the proton conductivity cell [13].

There are two components known prior to this, which are compartment A and compartment B. For this study, compartment A (VA = 50 cm^3) of the permeation cell was filled with methanol (CA = 1M). Meanwhile, compartment B was filled with distilled water instead. Both compartments were initially immersed into water for 24 hours. After that, the thickness of the hydrated membranes was measured three times to obtain an average thickness. It was then clamped between these two compartments. Methanol molecules eventually diffused through the membrane, along the gradient of concentration and into the opposite compartment of the permeation cell. Both compartments were then continuously stirred, and the concentration of methanol permeates in compartment A and B was measured using Pelkin Almer Flexar Liquid Chromatography. A linear standard curve of methanol concentration versus refractive index obtained from the methanol permeation test was organised to determine the methanol permeability of the membrane. P (methanol permeability) was calculated in accordance to the following equation:

$$P = \alpha \times \frac{V_B}{A} \times \frac{L}{C_A} \tag{5}$$

where, P stands for methanol permeability, $\alpha = (C_B(t)) / (t\text{-}t_o)$ refers to the slope of linear interpolation, with a focus on the plotting of methanol concentration in the permeate compartment, whereas V_B refers to the volume of the water compartment. Up next, A is the membrane cross-sectional area, L is the thickness of hydrated membrane and lastly, C_A is the concentration of methanol in the feed compartment [4]. In fact, there are desired membrane properties in achieving high performance direct methanol fuel cell (DMFC), such as having high proton conductivity, yet low methanol permeability. The overall membrane's characteristics can be obtained using the equation below:

$$\Phi = \frac{\sigma}{P} \tag{6}$$

The label Φ refers to a parameter that evaluates the overall membrane characteristics in terms of its ratio of proton conductivity, σ to methanol permeability, P. Whereas, for the thermal stability of the SPEEK/e-spun Cloisite15A® nanocomposite membrane, it was analysed by using a Mettler Todelo Thermogravimetric Analyzer (TGA/SDTA851e, Mettler-Toledo, International, Inc.). Approximately 6.42 mg of the sample was dried first at 210°C for 30 min to remove any moisture and then programmed at 0-600°C with a heating rate of 10°C/min under nitrogen atmosphere.

3. Results and discussion

3.1. Degree of Sulfonation SPEEK

Degree of sulfonation (DS) to SPEEK was determined by using the ^{1}HNMR analysis (Figure 2) and calculated based on Equation 1 as follows:

$$\frac{n}{12-2n} = \frac{\Delta H_{13}}{\sum \Delta H_{(integrated\ signal)}} \quad (0 \le n \le 1)$$

$$n = \frac{\Delta H_{13}}{\sum \Delta H_{(integrated\ signal)}} (12-2n)$$

$$n = \frac{12\Delta H_{13} - 2n\Delta H_{13}}{\sum \Delta H_{(integrated\ signal)}}$$

$$n = \frac{12\Delta H_{13}}{\sum \Delta H_{(integrated\ signal)} + 2\Delta H_{13}}$$

$$n = \frac{12(1)}{(6.374 + 10.746) + 2(1)}$$

$$n = 0.63$$

$$\therefore DS = n \times 100\% = 0.63 \times 100\% = 63\%$$

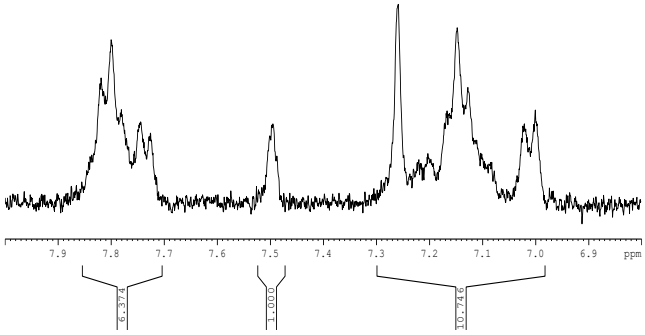

Fig. 2. H^{1}NMR spectra for SPEEK63.

3.2. Surface morphology study of the electrospun SPEEK63/Cloisite15A® nanofibers

A homogeneous formulation of the solution is important, especially the means of dispersion of Cloisite15A® which is an attempt to avoid agglomeration in the needle – an incident that may distort the formation of nanofiber. Nevertheless, many works of research have been done on preparing the homogenous electrospinnability inorganic dope solution and their success in spinning the solution [16-19]. However, the study in this particular field is rather limited. Thus, it is ensured that all Cloisite15A® particles in the syringe are fully electrospun and still present in nanofiber form, and all the homogeneous solution formulation needs to be spun at one time. With regards to the formulation of Cloisite 15A® solution, it was prepared by dissolving both Cloisite15A® and SPEEK63, acting as the carrier polymer in DMAc solvent.

To attain fine nanofibers for a targeted application, it is crucial to control the parameters of electrospinning and preparation of homogeneous dope formulation. However, it is seen as a failure if the nanofibers did not contain the aimed materials, for instance in this case, the Cloisite15A® particles. Moreover, introduction of filler (Cloisite15A®) to a charged polymer (SPEEK63) has increased the amount of interaction between the polymer chain and nanoclay, a combination that can isolate polymer chains within the amorphous region. Therefore, it is fundamental to carry out elemental analysis on the as-spun nanofibers by using EDX to further confirm the existence of Cloisite15A® particles. Figure 3 below shows the EDX mapping, specifically Silica (Si) of the prepared Cloisite15A® nanofibers. Based on the results, it can be clearly stated that Cloisite15A® was successfully electrospun and indeed present in the nanofiber mat. This remarkable achievement should be noted because no reports on similar findings have been documented thus far.

From Figure 3, the colour green indicates the presence of Cloisite15A® particles. It is observed that a considerably well distribution of Cloisite15A® clay was achieved. However, some of the Cloisite15A® clay layers were still intact with each other, forming a bulk yarn (as pointed out by the red arrow) due to the attractive force that dominantly developed around that particular area. This condition is closely related to the flocculated clay phenomenon, given that the attraction force was higher compared to the repulsive force, which eventually formed flocs. This occurs due to the fact that various forces tend to evolve between the submicroscopic-sized particles such as Cloisite15A® clay, whether it is attraction or repulsion [20].

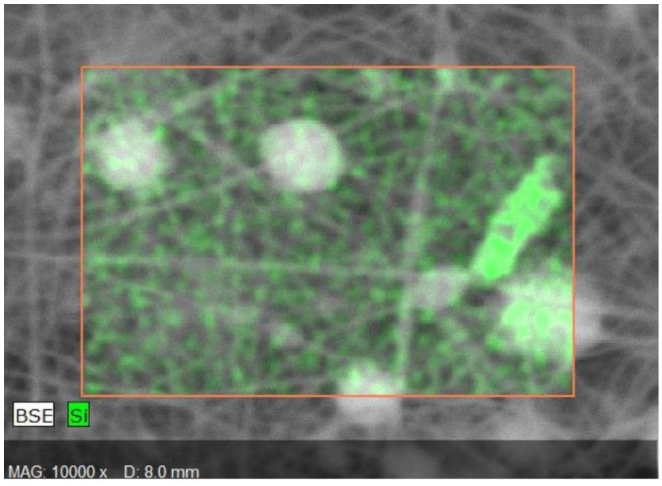

Fig. 3. EDX analysis of Silica (Si) mapping on as-spun Cloisite15A® nanofibers mat.

Fortunately, it is stated that this occurrence does not affect the conduction of proton. This is because proton transport can only rely on the existence of the ionic domain of the nanofiber structure, which allows the protons to be transported within PEM. As previously discussed by Mauritz and Moore [21], the orientation of the ionic domain along with the fiber axis direction can be achieved from a shear force during the electrospinning process. The aligned ionic structures have resulted in higher conductivity and this orientation can be extended if the convention of shear force increases, parallel to the decrease of fiber diameter.

3.3. Physical properties study of the electrospun SPEEK63/Cloisite15A® nanofibers

It is confirmed that the presence of Cloisite15A® filler within the electrospun nanofibers has proven that a good distribution of nanoclay can be achieved through the electrospinning method. However, the formation of beaded (indicated by the arrows) nanofibers as shown in Figure 4 a and b has always been considered as a defect, which could possibly affect the performance of the membrane. Since the feeding rate practiced in this study was 0.6 mL/hr, a considerably low feeding rate, the possibility of beaded nanofiber to form was more pronounced. At low feeding rate, the jet becomes unstable due to the fast ejection of dope solution and shift of mass-balance [22]. In fact, in their study, Neppalli et al. [23] had listed the effects of electrospinning on the polymorphism, structure and morphology of the poly (vinylidene fluoride) (PVDF) matrix through the introduction of Cloisite20A clay. It was found that the structure of fiber also depended on two types of forces, which are electrostatic and viscoelastic.

The elongation of the fiber was dependant on the electrostatic force. This is while the viscoelastic force affects the stretching of the fiber, which can lead to the formation of beads in the fiber and consequently increase the size of the diameter. Based on the SEM image in Figure 4 b, it can be said that the average diameter of SPEEK63/Cloisite15A® nanofibers is said to be in the range of 100-200 nm. A comparable diameter size was reported by Lee et al.

[24] , whereby their SPEEK67/SiO_2 nanofiber reached 232 nm. Since the obtained fibers were within the range of nanofiber diameter (62.5 nm to 375 nm), the as-spun SPEEK63/Cloisite15A® nanofibers produced in this study are considered as nanofibers with small diameter [24].

Inorganic nanofiber with small diameter can provide a large surface area to volume ratio, generating well-distributed inorganic fillers within the nanofiber-based electrolyte membrane. Subsequently, this could hinder the migration of methanol, besides allowing transportation of proton to pass through the membrane in DMFC operation. However, in this case study, the nanofiber structure was believed to be dissolved in DMAc during dope preparation and no longer present in the SPEEK63/e-spun CL nanocomposite membrane. Thus, both methanol permeation and performance of proton conductivity for the SPEEK63/e-spun CL nanocomposite membrane did not correlate with the listed characteristics of the nanofiber. The performance of SPEEK63/e-spun CL nanocomposite membrane will be explained in detail in the next section.

3.4. Dispersion state of cloisite15A® in SPEEK63/e-spun CL nanocomposite membrane

The contribution of electrospinning on the nanocomposite membrane's morphological structure is expected to bring together the formation of an exfoliated nanocomposite membrane – given that the polymer-based silicate membrane is separated by individual clay layers in a continuous polymer matrix by an average distance, depending on the clay loading. In fact, it is expected to occur at lower clay loading compared to phase separation and the intercalated nanocomposite membrane [25]. Hence, to determine the morphological structure of the nanocomposite membrane, whether it was exfoliated, intercalated or within a phase of separation, the x-ray diffraction (XRD) test was performed. To enlighten, XRD measures the degree of particle dispersion by estimating the distance between individual platelets after mixing with polymer. Any changes to the interlayers of clay due to polymer intercalation can indeed cause changes in position, broadness and intensity of the diffraction peak in XRD spectra [26].

As discussed earlier, there are three varying conditions for particles dispersion to occur within the polymer matrix: (1) phase separation, (2) intercalation or (3) exfoliation. First off, phase separation nanocomposite ensues when the diffraction peak of interlayers shows angles equal or higher than the pure clay itself. Intercalation nanocomposite however, occurs when the diffraction peak shows an increase of spacing in between the mentioned interlayers instead. Although the peak was not seen in diffractograms, an exfoliated nanocomposite was still obtained. Although, when the peak broadened, it hinted the presence of a partially exfoliated nanocomposite membrane within the polymer matrix.

In this case study, in retrospection to our previous report, the analysis of pure Cloisite15A® has shown corresponding basal distance planes of 0.01 at $2\Theta = 7.1°$ with a gallery recorded distance of 1.24 nm. For further clarification, another peak was correspondingly observed: whereby the pure Cloisite15A® recorded at $2\Theta = 2.6°$ is shown in Figure 5 a. This peak indicates the presence of tallow molecules within the clay structure. In addition, very little SPEEK63 had also intercalated into the gallery space [27]. Figure 5 c conversely shows that the gallery distance has shifted to a lower angle; from $2\Theta = 7.1°$ to $2\Theta = 6.02°$, further demonstrating the formation of the intercalated nanocomposite membrane. Though a comparable pattern was initially found by Jaafar et al. [28] on SPEEK/CL. even at $2\Theta = 2.6°$, the diffraction pattern showed a much lower reading compared to pure Cloisite15A®. Such behaviours may have occurred due to the presence of intercalation of clay in the polymer matrix, as repeatedly mentioned before. In addition, Figure 5 b shows no sign of peak when observed at $2\Theta = 7.1°$, compared to Figure 5 c, in which its reading may be impacted from the absence of Cloisite15A®.

It is understood that the dispersion state of inorganic fillers in nanoscale has a positive impact on the performance of the polymer electrolyte composite-based membrane – inclusive proton conductivity and methanol permeability. This is most likely the effect of capacity enlargement of mobile cations for proton conductions, thus providing critical tortuosity towards methanol pathways. From this study, it is found that the employment of the electrospinning technique has indeed contributed to the improvement of normal composite towards the intercalated dispersion state of inorganic fillers (Cloisite15A® clay) in nanosized scale. Owning up to its promising and reliable advantages towards producing nanoscale fibers, the electrospinning technique is used to achieve the target put forth. Such a sea of knowledge should be explored to improve both precision and properties of the electrospun fiber for it to be up to industrial scale.

As for the formation of a SPEEK63/ Cloisite15A® nanocomposite membrane in this study, it does differ greatly from several previously studied membranes, especially in terms of its method and state of clay distribution (refer to Table 3). Even though SPEEK63/e-spun CL did exhibit an intercalated structure, the intensity of its peak is low and almost diminished. Nevertheless, it is established that the intercalated SPEEK63/e-spun CL structure was indeed obtained. By electrospinning the Cloisite15A® particle, its size had successfully reduced by 65% when compared to the average size commonly found in the SPEEK63/2.5CL/5.0TAP membrane (within the range of 20 -160 nm).

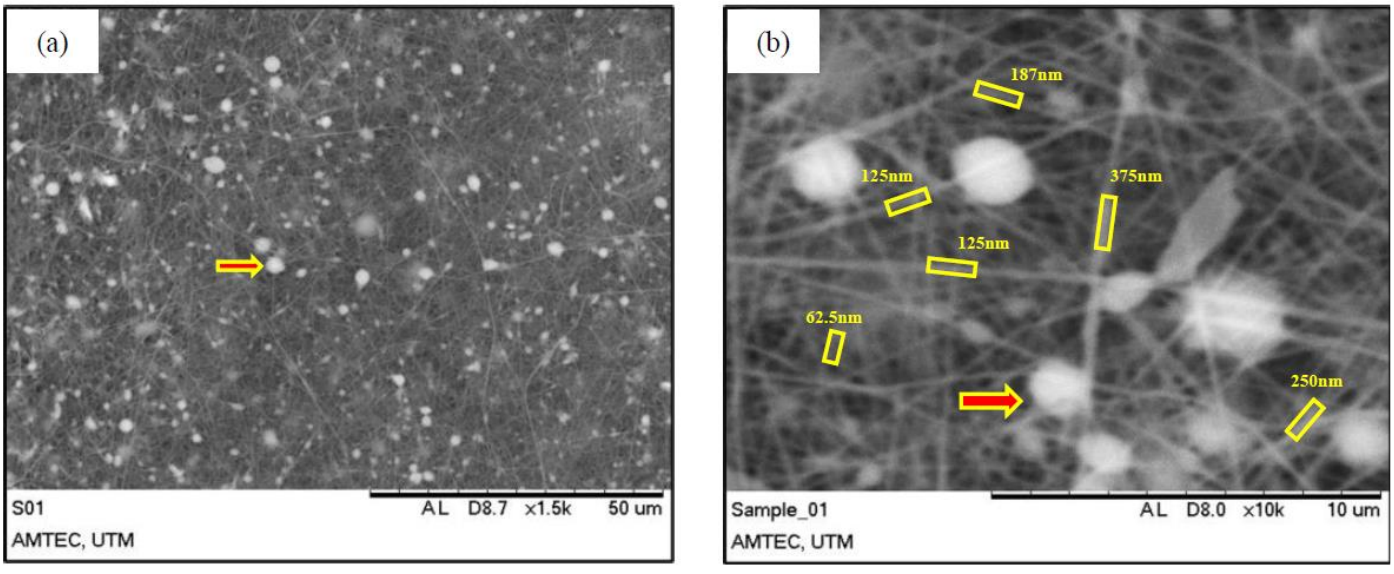

Fig. 4. SEM images of Cloisite15A® nanofiber with (a) low magnification, 1.5k, and (b) higher magnification, 10k.

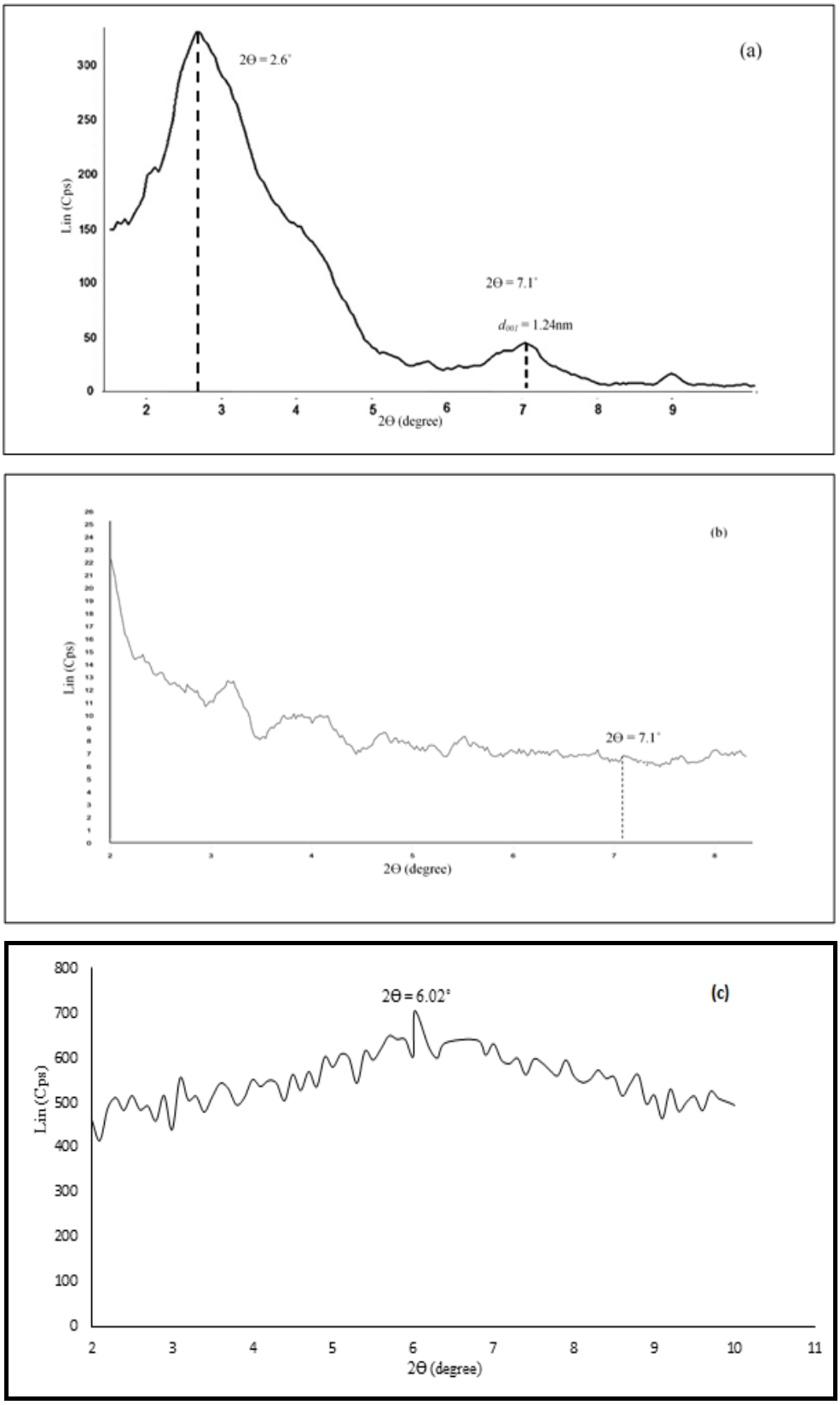

Fig. 5. XRD patterns of (a) Cloisite15A®, (b) SPEEK63 and (c) SPEEK63/e-spun CL nanocomposite membranes.

Although the intercalated clay was given utmost attention to, it did not hinder the study's main purpose: which is to reduce the size of Cloisite15A® particle distributed in membrane polymer matrices. On the other hand, Cloisite15A® in SPEEK63/e-spun CL was found to fall within the range of 19.9 – 55.9 nm (Figure 6), concluding that inorganic filler was successfully dispersed within the electrospun fiber, being simultaneously reduced to nanometer. When compared to Figure 9, the most dominant size of Cloisite15A® was within the range of 19.9 nm. The intercalated structure morphology for the prepared membrane is believed to have affected the selectivity of the membrane in terms of both proton conductivity and methanol permeability.

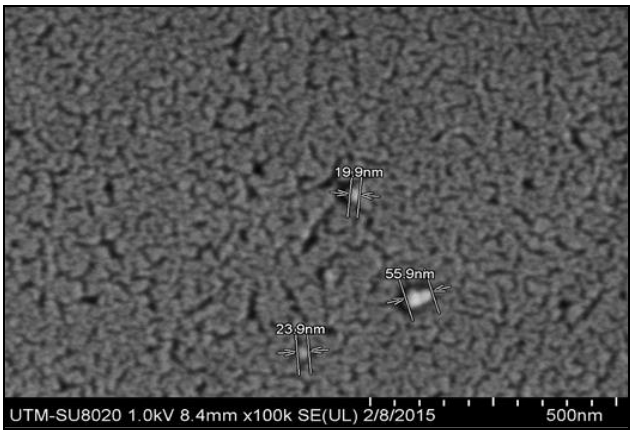

Fig. 6. FESEM image of Cloisite15A® nanoclay size distribution in SPEEK63/e-spun CL nanocomposite membrane.

Table 3
Methods in preparing SPEEK63/ Cloisite15A® nanocomposite membrane.

Sample	Method	Clay distribution
SPEEK63/2.5CL/5.0TAP [13]	Solution intercalation method + compatibilizer	Exfoliated
SPEEK63/e-spun CL	Solution intercalation method + electrospinning process	Intercalated

Based on the findings from studies discussing SPEEK63/e-spun CL and SPEEK63/2.5CL/5.0TAP, it can be concluded that an exfoliated membrane structure has more impact towards the formation of tortuosity pathway for methanol migration through the membrane. Meanwhile, the beneficial impact of the intercalated membrane structure is more so to induce proton conduction [4]. Figure 7 depicted the pathway of protons (H^+) and methanol molecules within the exfoliated and intercalated structure, respectively.

From Figure 7 (a), it was suggested that the contribution of nanovoids between Cloisite15A® nanoparticles in the polymer matrix and the presence of TAP has indeed increased both proton conductivity and the tortuous pathway for methanol permeation. It is common to achieve higher activity of proton conduction in the nanocomposite electrolyte membrane, especially when having well-dispersed inorganic fillers. With that being said, the contribution of smaller-sized particles of frequently mentioned inorganic fillers could provide a substantial improvement in proton conductivity, as well as methanol permeability. The presence of nanovoids has provided a sieving effect for the methanol pathway. Simultaneously, it has led methanol molecules to travel on a high aspect ratio of clay platelet, thus creating a winding diffusion pathway for methanol. Meanwhile, a proton (H^+) atom freely flows through the nanovoids due to "proton hopping", allowing it to hop from one molecule to another (Cloisite15A®).

Even though methanol permeability is recorded higher in the intercalated membrane (Figure 7 b), this membrane has contributed to a higher proton conductivity value in comparison to the exfoliated SPEEK63/2.5CL/5.0TAP membrane. This phenomenon ensued due to the contribution of the electrospinning process on the volume of Cloisite15A®. The reduction on its size may attribute to higher dispersion, all the while allowing more protons to be transferred. That being said, higher methanol permeability could also be prompted due to large nanovoids formed between Cloisite15A® nanoclay vicinities. As the size of Cloisite15A® decreases, larger nanovoids are formed, which are depicted in Figure 8.

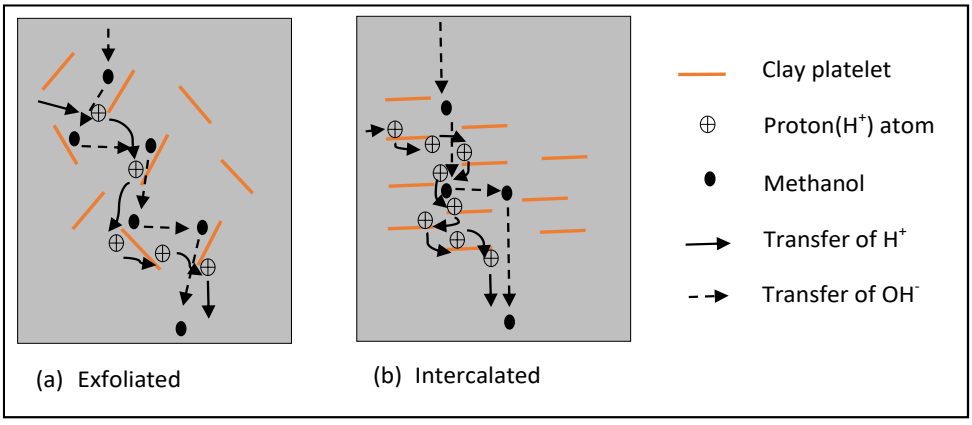

Fig. 7. Models for proton and methanol transport within nanocomposite matrix structure (a) exfoliated SPEEK63/2.5CL/5.0TAP and (b) intercalated SPEEK63/e-spun CL.

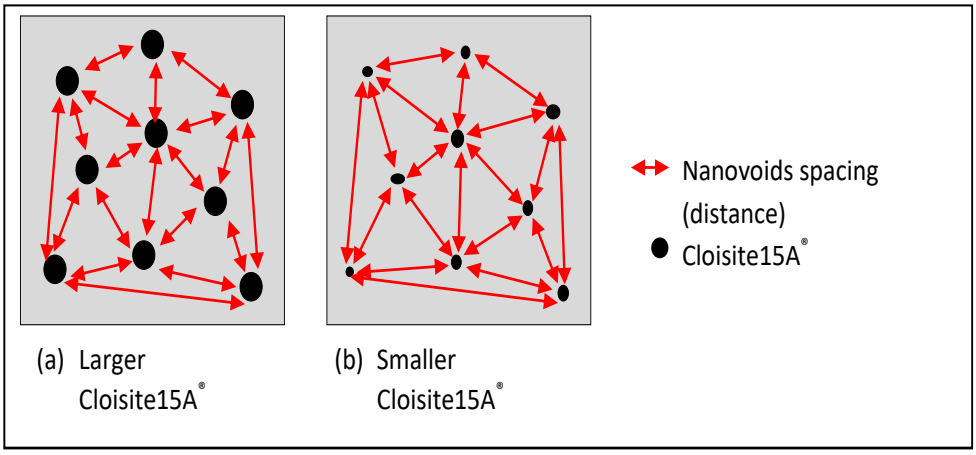

Fig. 8. Models of nanovoids spacing of (a) larger Cloisite15A® nanoparticles and (b) smaller Cloisite15A® nanoparticles.

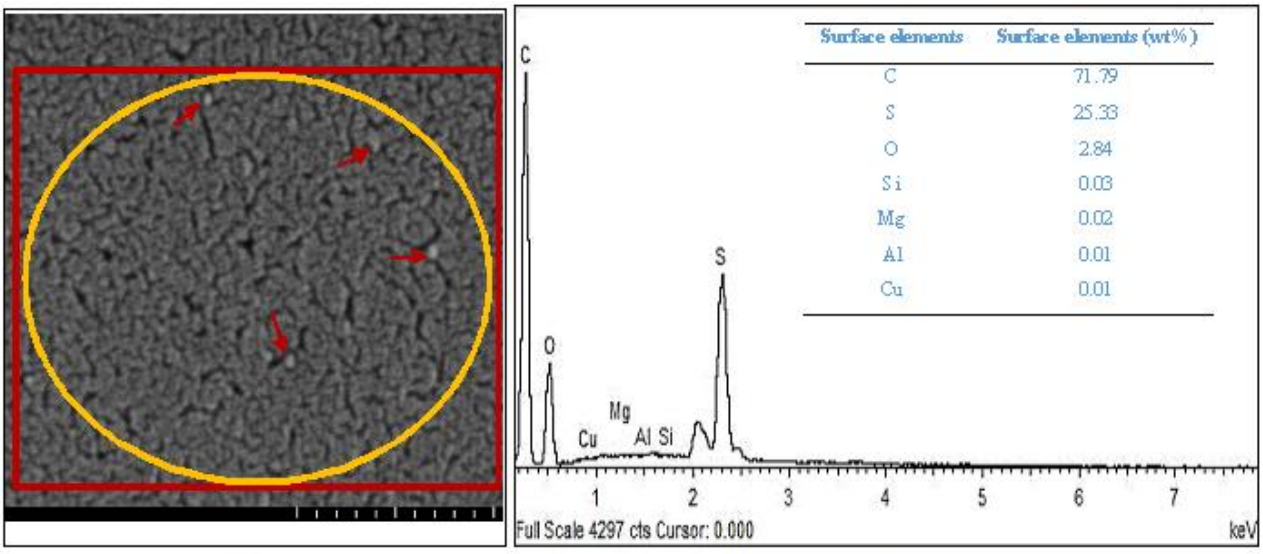

Fig. 9. FESEM images of (a) EDX mapping and (b) EDX spectra analysis on surface micrograph of SPEEK63/e-spun CL nanocomposite membrane.

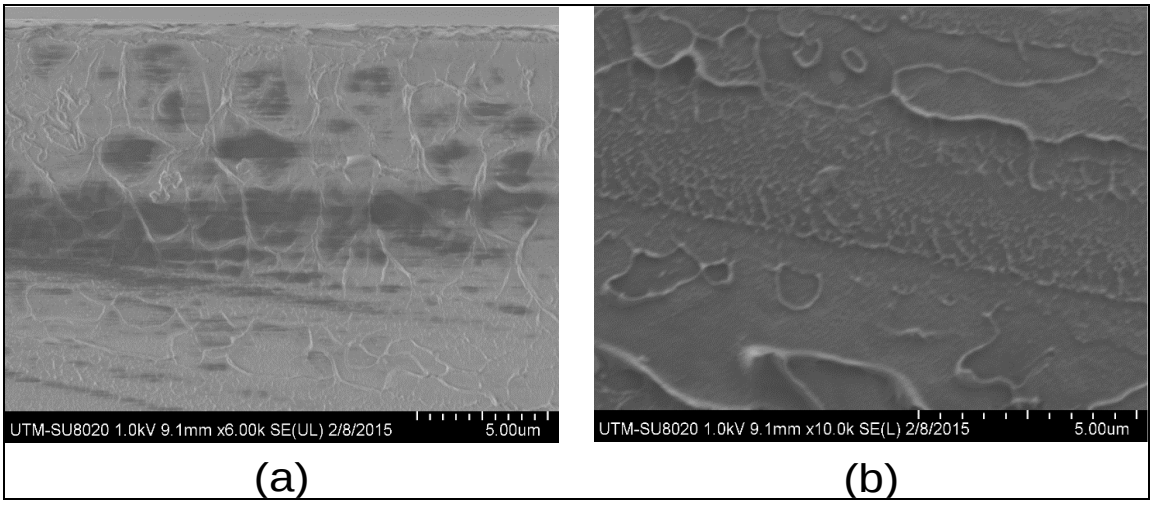

Fig. 10. FESEM images on cross-section surface of SPEEK63/e-spun CL nanocomposite membranes at (a) low magnification, 6k and (b) high magnification, 10k.

3.5. Morphological structural study on SPEEK63/e-spun CL nanocomposite membrane

FESEM images of EDX mapping on the surface micrograph of SPEEK63/e-spun CL nanocomposite membranes are presented in Figure 9. The EDX spectrum of SPEEK63/e-spun CL nanocomposite fiber is shown in Figure 9 b instead, confirming the presence of Cloisite15A®. This is while Figure 10 a and b displays the FESEM images of the membrane cross-section at lower and higher magnification. From Figure 9 a, the arrows on the image itself point out particles of Cloisite15A® within the SPEEK63 nanocomposite membrane. At this magnification, there was only a small amount of Cloisite15A® particles found. This image is proportional with the data in Figure 9 b since a lower peak was present for silicon (Si). However, from this observation, it can be stated that a good distribution of Cloisite15A® particles was present all over the membrane surface.

As previously discussed, the clay itself tends to be intact from the attraction or force of repulsion. This may also lead to the formation of fracture or defect on the membrane surface as can be seen in Figure 9. Nevertheless, the observation on the cross-sectional area (Figure 10) concluded that the formation of a dense SPEEK63/e-spun CL nanocomposite membrane was established.

3.6. Thermal stability of SPEEK63/e-spun CL nanocomposite membrane

The thermogravimetric analysis (TGA) was used in order to determine the thermal stability of the SPEEK63/e-spun CL nanocomposite membrane and the fraction of its volatile component after being heated at a certain temperature by monitoring the changes of weight percentage of the components. In this study, it is important to evaluate the TGA of the membrane, given that it will determine the temperature it withstands for usages in DMFC, operating up to 120°C. Figure 11 illustrates the TGA profiles for the SPEEK63/e-spun CL nanocomposite membrane. It indicates that the membrane started to degrade at a temperature of 0°C - 150°C. The mentioned thermal degradation occurs when the membrane loses water during the sulfonation process. When the temperature increased up to 350°C, it evidently showed that the membrane went under another thermal degradation, since the sulfonic acid group had been decomposed at this exact temperature. A similar observation was reported by Sakaguchi et al. [29]. The sample undertook the third stage of thermal degradation at the midpoint temperature of 550°C, which is attributed to the release of olefin and amine of Cloisite15A® nanoclay. Based on the stability of each material in the membrane at a high degree that exceeded the DMFC operating temperature (ranging from 60°C to 120°C), it can be suggested that the prepared SPEEK63/e-spun CL nanocomposite membrane is suitable to be used in DMFC.

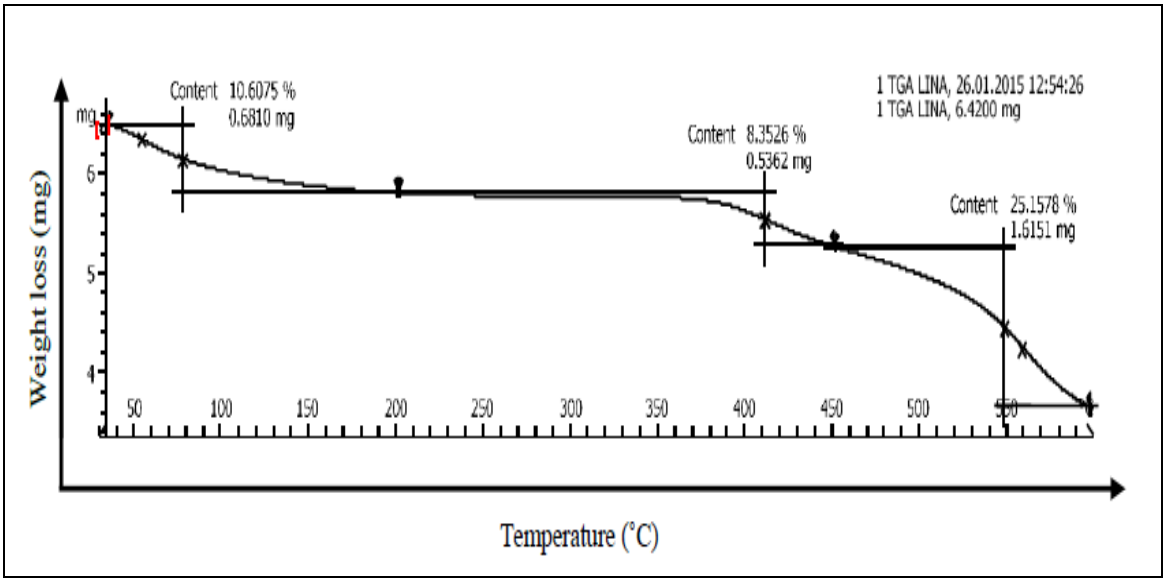

Fig. 11. TGA curve for SPEEK63/e-spun CL nanocomposite membrane.

3.7. Physical properties of SPEEK63/e-spun CL nanocomposite membrane

All the results of characterisation to SPEEK63/e-spun CL nanocomposite membrane is compared to SPEEK63-based membranes, ones that have been previously developed. As a matter of fact, it is crucial to note that a thorough comparison between the two was made on the basis of a different approach in depositing Cloisite15A® nanoclays, to provide a homogeneous polymer-clay nanocomposite membrane. Electrospinning was likewise integrated in the SPEEK63/e-spun CL fabrication, whereas a compatibiliser was utilised in preparing the SPEEK63/2.5CL/5.0TAP membrane. All in all, it is significant to investigate how far the electrospinning approach could contribute to providing a promising polymer-clay based electrolyte membrane for DMFC applications. Table 4 tabulates the comparative study on SPEEK63/e-spun CL and other types of SPEEK63, as well as Nafion112 provided from the previous study.

Table 4
Formulation of designed proton electrolyte membrane (PEM).

Membrane designation	Thickness (cm)	*Degree of sulfonation (DS) (%)	Amount of SPEEK (%)	Amount of Cloisite15A (%)
Nafion112 [4]	0.0060	NA	NA	NA
SPEEK63 [4]	0.0060	63	10	NA
SPEEK63/2.5 CL/5.0TAP [4]	0.0071	63	10	2.5
SPEEK63/e-spun CL	0.0069	63	16	0.05

**The DS was taken as the DS of the synthesized SPEEK63 polymer before dope formulation preparation.*

3.7.1. Water uptake

The correlation between water uptake and proton conductivity is inevitable as the water absorbed by the polymer electrolyte membrane acts as a medium to facilitate proton transport. This brings us to a conclusion whereby high-water uptake is favourable for proton conduction activity. Unfortunately, it did seem to encourage methanol crossover which can be taxing and cause a decline in its performance under DMFC operation. Therefore, an appropriate amount of water absorption is necessary to obtain the polymer electrolyte membrane with acceptable performance characteristics. Table 5 shows the comparative study on water uptake of SPEEK63/e-spun CL to that of different polymer electrolyte membranes obtained from the previous study.

Table 5
Water uptake of the prepared SPEEK63/e-spun CL membrane in comparison to Nafion 112, SPEEK63, and SPEEK63/2.5CL/5.0TAP as the reference membranes.

Membrane Designation	Water Uptake (wt. %) (*n*=3)
Nafion 112 [4]	21.43 ± 0.74
SPEEK63 [4]	29.70 ± 0.10
SPEEK63/2.5CL [4]	54.87±0.07
SPEEK63/2.5CL/5.0TAP [4]	26.19 ± 0.27
SPEEK63/e-spun CL	19.00 ± 0.21

**n is the number of repetition*

From Table 5, it can be stated that the contribution of sulfonic acid group has led to the highest value of water uptake for SPEEK63 membrane, as compared to the commercialised Nafion112 and SPEEK63-based nanocomposite membranes. The intrinsic feature of high hydrophilicity of SPEEK has contributed to the greater ability of the membrane in absorbing more water molecules. However, the inclusion of both Cloisite15A® (CL) and triaminopyrimidine (TAP) to the SPEEK63 matrix has reduced its capability in absorbing water molecules. In Jaafar et al.'s study, it was believed that this phenomenon occurred due to the compact polymer chain that eventually reduced the movement of polymer, as well as the free voids in the nanocomposite membrane [4]. This was subsequently supported by Pluart [30], whereby he found that involvement of the exfoliated structure has contributed to high aspect ratio, thus constructing a tortuous pathway for even water to diffuse. Meanwhile, the resultant SPEEK63/e-spun CL nanocomposite membrane from this study has shown a dramatic drop in water uptake by approximately 26% that of the SPEEK63/2.5CL/5.0TAP membrane. At first sight, this drop is believed to significantly reduce the overall performance of the membrane.

Albeit so, it has been proven that Cloisite15A® itself can absorb and reserve water molecules with the presence of hydrophilic group (OH^-) in its structure [31], allowing hydrogen to bond with water molecules and ultimately increase the water uptake of parent SPEEK63 – as can be seen in Table 5 on the SPEEK63/2.5CL membrane. It is also fascinating that the contribution of electrospinning in this study has led to the low value of water uptake as compared to SPEEK63/2.5CL. The smaller inorganic fillers produced from the electrospinning process were believed to reduce the capability of Cloisite15A®, specifically to hold the water molecules in such a big amount. With the contribution of the hydrophobic surface of Cloisite15A® on the intermolecular interaction of the water surface, it has led to low permeability of water within the nanocomposite membrane. At this point, by considering both cases, it can be concluded that other than electrospinning's contribution in reducing the size of Cloisite15A® from mixed (nm and μm) to nm size range, the clay itself is capable of decreasing the water uptake of the composite membrane.

3.7.2. Proton conductivity

An excellent fuel cell system requires both high fuel barrier properties and proton conductivity for it to fulfil industrial expectations. Particularly for DMFC, a proton electrolyte membrane (PEM) with lower methanol permeability and high proton conductivity is fundamental. A comparative figure was designed as below to show the comparable value of proton conductivity of Nafion112, SPEEK63, SPEEK63/2.5CL/5.0TAP and SPEEK63/e-spun CL. Figure 12 indicates that the SPEEK63/e-spun CL possessed the highest proton conductivity when compared to other Nafion112, SPEEK63 and SPEEK63/2.5CL/5.0TAP membranes. In fact, the contribution of electrospinning on Cloisite15A® size reduction is believed to have caused fillers to aggregate to some extent that lead to a continuous conduction pathway for the proton to transfer [32]. This was formed in parallel with the contribution of Cloisite15A® nanoclay, one that holds proton molecules, yet increases the value of proton conductivity. From the results shown in Table 5, it is also understood that the water uptake is not directly correlated to proton conductivity of the membrane. Generally speaking, the transportation occurred by two different mechanisms (Grotthuss and vehicle mechanisms) that reflected different outcomes, whereby in this present study, the Grotthuss mechanism was more dominant. This is because the transport of proton occurred along the hydrogen bond network of Cloisite15A® and SPEEK was done in a shortened distance via proton hopping, compared to the vehicle mechanism which usually contributes to an increase of water uptake instead [33].

3.7.3. Methanol permeability

Other than that, methanol permeability has also piqued some interest in DMFC application since it can hinder DMFC's good performance. Formerly, several approaches had been introduced to cater the problem in regards to methanol crossover [34]. One of the foremost approaches is introducing nanocomposite into the polymer matrix. From a previous study, it had been proven that the introduction of Cloisite15A® within the SPEEK63 matrix decreases the value of methanol permeability in the DMFC application. The changes of methanol permeation rate in retrospect to time (seconds) of the prepared SPEEK63/e-spun CL nanocomposite membrane, Nafion112, SPEEK63 and SPEEK63/2.5CL/5.0TAP are shown in Figure 13. For SPEEK63/e-spun CL, its methanol permeability was recorded 3 times higher than SPEEK63/2.5CL. This could probably be due to the cracks on the membrane structure, which led to bigger molecules such as methanol to escape. Likewise, the low loading of Cloisite15A® that hindered the ability of Cloisite15A®, acts as an obstacle for polymer mobility. Nevertheless, from this observation, it is proven that Cloisite15A® can decrease the methanol permeability compared to SPEEK63/e-spun CL with Nafion 112.

It shows that the contribution of Cloisite15A® is parallel with the research done by Jaafar et al., stating that the high aspect ratio with higher surface area resulted from adequate filler loading can provide a tortuous pathway for methanol crossover, simultaneously hindering methanol permeation [28]. Yet, by realizing that the well dispersion of Cloisite15A® seems promising in reducing the methanol permeability of the SPEEK63 membrane, it is vital to compare the values of methanol permeability values between SPEEK63/e-spun CL and SPEEK63/2.5CL (prepared by simple blending method) membranes. After close observation, it clearly shows that the employment of electrospinning has indeed improved the vicinity of Cloisite15A® nanoclays. As what has been discussed earlier, the permeation of methanol in SPEEK63/e-spun CL was recorded higher than SPEEK63/2.5CL, relatively greater than others, except for Nafion112 that was attributed to the formation of nanovoids between adjacent nanoclays [30].

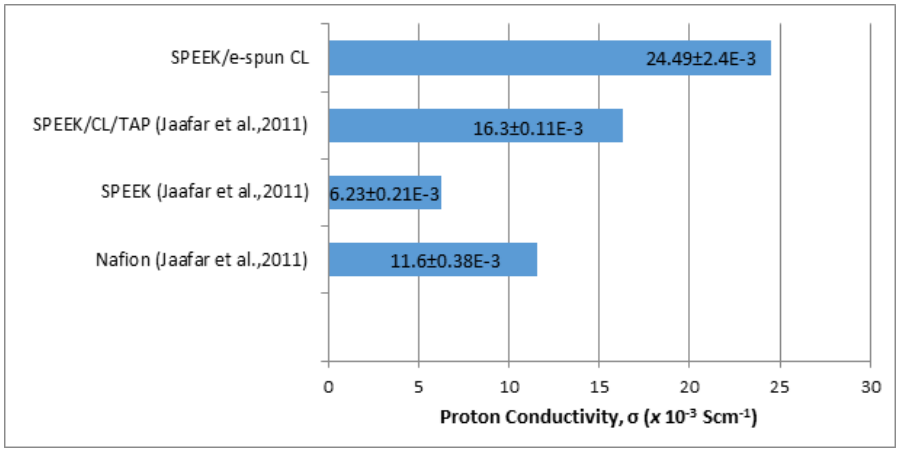

Fig. 12. Comparative study on proton conductivity of Nafion112, SPEEK63, SPEEK63/2.5CL/5.0TAP and SPEEK63/e-spun CL.

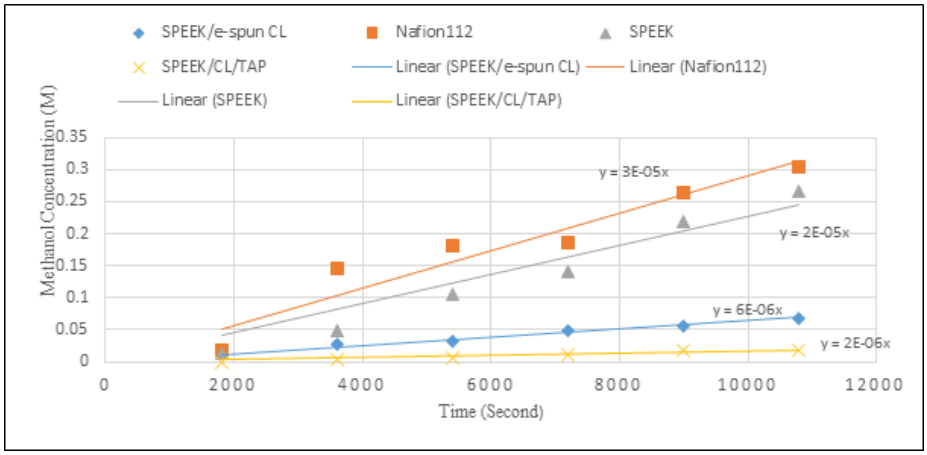

Fig. 13. Methanol permeation rate of other different types of SPEEK63 membranes and Nafion112 membranes.

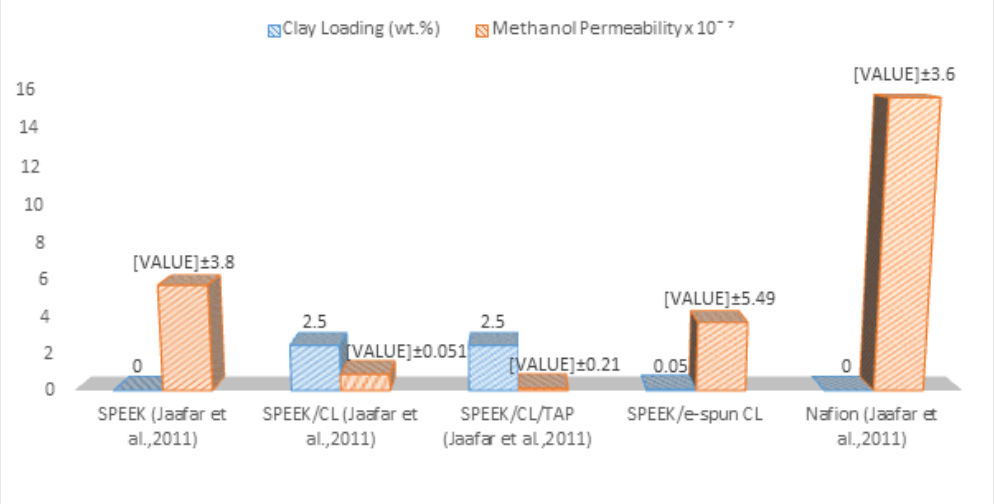

Fig. 14. Clay loading and the methanol permeability for different types of SPEEK63 membranes.

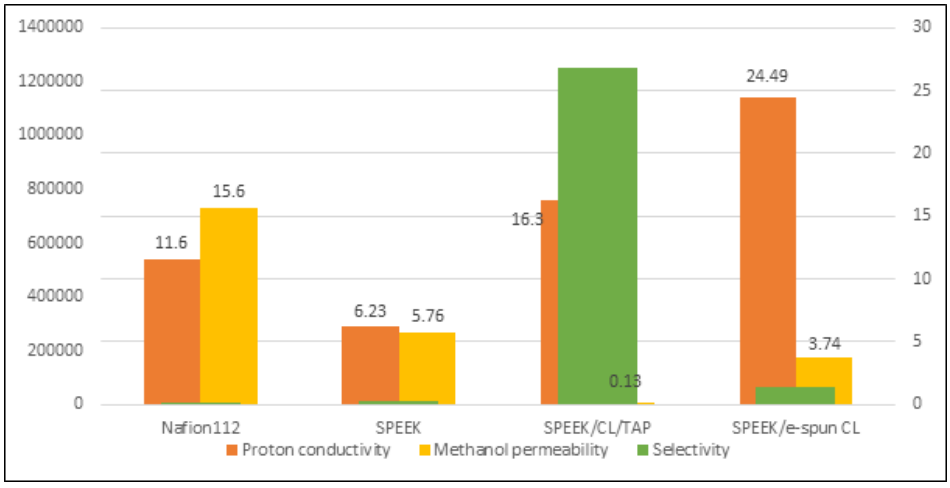

Fig. 15. Overall performance of polymer electrolyte membrane.

3.7.4. Membrane selectivity

Excellent membrane selectivity should contribute to an outstanding performance of polymer electrolyte membrane (PEM). This PEM should possess great characteristics in relation to proton conductivity, and low methanol permeability to perform high selectivity. These two factors theoretically contribute to the high performance of PEM in real DMFC application. Table 6 shows the performance of SPEEK63, SPEEK63/2.5CL/5.0TAP, Nafion112 and SPEEK63/e-spun CL in terms of its respective proton conductivity and methanol permeability. The output ratios formed from those characteristics will yield the overall membrane characteristics or selectivity and are illustrated in Figure 15.

Table 6
Performance of SPEEK63, SPEEK63/2.5CL/5.0TAP, Nafion112 and SPEEK63/e-spun CL.

Sample	Proton conductivity, $\sigma\,(x\,10^{-3} Scm^{-1})$	Methanol permeability ($x\,10^{-7}\ cm^2/s$)	Overall membrane characteristic
Nafion112 [4]	11.6 ± 0.38	15.6 ± 3.6	7435.90
SPEEK63 [4]	6.23 ± 0.21	5.76 ± 3.8	10834.78
SPEEK63/2.5CL/5.0TAP [4]	16.3 ± 0.11	0.130 ± 0.21	1253846.15
SPEEK63/e-spun CL	24.49 ± 2.4	3.74 ± 5.49	65481.28

By commencing electrospinning, it can increase the proton conductivity up to 50% higher than SPEEK63/2.5CL/5.0TAP. This is while methanol barrier properties of SPEEK63/e-spun CL were recorded lower compared to SPEEK63/2.5CL/5.0TAP. However, it is important to highlight that the addition of a very small amount of Cloisite15A® (0.05wt.%) in SPEEK63/e-spun CL has significantly enhanced the proton conductivity of the membrane, unlike the 2.5wt.% Cloisite15A® loading in the SPEEK63/2.5CL/5.0TAP membrane. Based on the findings obtained, it is concluded that electrospinning has contributed to the smaller dimension of Cloisite15A®, eventually resulting in higher conductivity of the membrane, by adding to the contribution of conductive features. Aside from that, it can also be deduced that the low loading of Cloisite15A® has contributed to low methanol barrier properties, one of the most important part in DMFC. However, the low loading of the filler is not the only factor that contributes to low methanol barrier properties, given that the morphology structure of the membrane, particularly its dispersion state of inorganic fillers, also affect the pathway for methanol to travel as previously discussed.

4. Conclusions

The nanocomposite membrane which is composed of sulfonated poly (ether ether ketone) (SPEEK) and e-spun Cloisite15A® was successfully prepared. From this study, it is found that the employment of the electrospinning technique has indeed contributed to improving the normal composite towards the intercalated dispersion state of the inorganic fillers

(Cloisite15A® clay) in nanosized scale. However, it also contributed to a good distribution of Cloisite15A® particles throughout the nanocomposite membrane surface. Owing to its promising and reliable advantages towards producing nanoscale fibers, the electrospinning technique has successfully decreased the particles size of Cloisite15A® up to nanometer sizes in conjunction with acceptable selectivity of the membrane. In addition, it is found that the impregnation of e-spun Cloisite15A® into the SPEEK matrix has increased proton conductivity with an acceptable value of methanol permeability for the DMFC application. Thus, it was suggested that these new polymer electrolyte nanocomposite membranes have a high potential to be used in DMFC operations with a temperature range of 60 -120 °C.

5. Acknowledgement

The authors are thankful to the Ministry of Science, Technology and Innovation Malaysia (MOSTI), Ministry of Education (MOE) and Universiti Teknologi Malaysia under Research University Grant Scheme (Project Number: Q. J130000.2546.13H51 and Q. J130000.2546.12H56). The authors would also like to acknowledge technical and management support from Research Management Centre (RMC), Universiti Teknologi Malaysia.

References

[1] Y.I. Tien, K.H. Wei, Hydrogen bonding and mechanical properties in segmented montmorillonite/polyurethane nanocomposites of different hard segment ratios, Polym. J. 42 (2001) 3213-3221.

[2] M. Wang, S. Dong, Enhanced electrochemical properties of nanocomposite polymer electrolyte based on copolymer with exfoliated clays, J. Power Sources 170 (2007) 425-432.

[3] Y.S. Choi, T.K. Kim, E.A. Kim, S.H. Joo, C. Pak, Y.H. Lee, H. Chang, D. Seung, Exfoliated sulfonated poly (arylene ether sulfone)-clay nanocomposites, Adv. Mater. 20 (2008) 2341-2344.

[4] J. Jaafar, A.F. Ismail, T. Matsuura, and K. Nagai, Performance of SPEEK based polymer–nanoclay inorganic membrane for DMFC, J. Membr. Sci. 382 (2011) 202–211.

[5] F. Croce, G.B. Appetecchi, L. Persi, B. Scrosati, Nanocomposite polymer electrolytes for lithium batteries, Nature 394 (1998) 456-458.

[6] D. Golodnitsky, G. Ardel, E. Peled, Ion-transport phenomena in concentrated PEO-based composite polymer electrolytes, Solid State Ionics 47 (2002) 141-155.

[7] A. Zucchelli, D. Fabiani, C. Gualandi, An innovative and versatile approach to design highly porous, patterned, nanofibrous polymeric materials, J. Mater Sci. 44 (2009) 4969-4975.

[8] D. Zhang, A.B. Karki, D. Rutman, D.P. Young, A. Wang, D. Cocke, T.H. Ho, and Z. Guo, Electrospun polyacrylonitrile nanocomposite fibers reinforced with Fe_3O_4 nanoparticles: fabrication and property analysis, Polym. J. 50 (2009) 4189–4198.

[9] J. Fang, X. Wang, T. Lin, Functional applications of electrospun nanofibers, in: T. Lin (Ed.), Nanofibers-production, properties and functional applications, InTech, Croatia, 2011, pp. 287-326.

[10] S. Cavaliere, S. Subianto, I. Savych, D.J. Jones, J. Rozière, Electrospinning: designed architectures for energy conversion and storage devices, Energy Environ. Sci. 4 (2011) 4761–4785.

[11] B.P. Sautther, Continuous polymer nanofibers using electrospinning, NSF-REU Summer 2005 Program, Universities of Illinois, Chicago, 2005.

[12] V. Thavasi, G. Singh, S. Ramakrishna, Electrospun nanofibers in energy and environmental applications, Energy Environ. Sci. 1 (2008) 205-221.

[13] M.W. Cason, Electrospun nafion® nanofibers for proton exchange membranes, Literature Seminar, 2010, 23 September.

[14] D. Thompsett, Recent developments in electrocatalyst activity and stability for proton exchange membrane fuel cells, in D.P. Wilkinson, J. Zhang, R. Hui, J. Fergus, X. Li (Eds.), Proton exchange membrane fuel cells: materials properties and performance, CRC Press, 2009, pp. 1-60.

[15] M.H.D. Othman, A.F. Ismail, A. Mustafa, Physico-chemical study of sulfonated poly (ether ether ketone) membranes for direct methanol fuel cell application, Malay. Polym. J. 2 (2007) 10-28.

[16] Z. Hongwei, Y. Fei, Z. Danying, Fabrication and characterization of electrospun sulfonated poly (phthalazinone ether ketone) mats as potential matrix of reinforced proton exchange membranes, J. Appl. Polym. Sci. 130 (2013) 4581-4586.

[17] I. Shabani, M.M. Hasani-Sadrabadi, V. Haddadi-Asl, M. Soleimani, Nanofiber-based polyelectrolytes as novel membranes for fuel cell applications, J. Membr. Sci. 368 (2011) 233-240.

[18] S. Mollá, V. Compañ, Polyvinyl alcohol nanofiber reinforced Nafion membranes for fuel cell applications, J. Membr. Sci. 372 (2011) 191-200.

[19] M.M. Hasani-Sadrabadi, E. Dashtimoghadam, K. Sarikhani, F. S. Majedi, G. Khanbabaei, Electrochemical investigation of sulfonated poly (ether ether ketone)/clay nanocomposite membranes for moderate temperature fuel cell applications, J. Power Sources 195 (2010) 2450-2456.

[20] H. van. Olphen, Forces between suspended bentonite particles. Shell Development Company, Houston, Texas, 1956, pp. 204-224.

[21] K.A. Mauritz, R.B. Moore, State of understanding of Nafion. Chem. Rev. 104 (2004) 4535-4585.

[22] R. Jalili, S.A. Hosseini, M. Morshed, The effects of operating parameters on the morphology of electrospun polyacrylonitrile nanofibers, Iran. Polym. J. 14 (2005) 1074–1081.

[23] R. Neppalli, S. Wanjale, M. Birajdar, V. Causin, The effect of clay and of electrospinning on the polymorphism, structure and morphology of poly (vinylidene fluoride), Eur. Polym. J. 49 (2013) 90-99.

[24] C. Lee, S.M. Jo, J. Choi, K.-Y. Baek, Y.B. Truong, I.L. Kyratzis, Y.G. Shul, SiO_2/sulfonated poly ether ether ketone (SPEEK) composite nanofiber mat supported proton exchange membranes for fuel cells, J. Mater. Sci. 48 (2013) 3665-3671.

[25] S.S. Ray, M. Okamoto, Polymer/layered silicate nanocomposites: a review from preparation to processing, Prog. Polym. Sci. 28 (2003) 1539-1641.

[26] A. Olad, Polymer/clay nanocomposites, in: B. Reddy (Ed.), Advances in diverse industrial applications of nanocomposites, InTech, Croatia, 2011, pp. 113-139.

[27] G.D. Barber, B.H. Calhoun, R.B. Moore, Poly (ethylene terephthalate) ionomer-based clay nanocomposites produced via melt extrusion, Polym. J. 46 (2005) 6706-6714.

[28] J. Jaafar, A.F. Ismail, T. Matsuura, Preparation and barrier properties of SPEEK/Cloisite 15A®/TAP nanocomposite membrane for DMFC application, J. Membr. Sci. 345 (2009) 119–127.

[29] Y. Sakaguchi, K. Kitamura, J. Nakao, S. Hamamoto, H. Tachimori, S. Takase, Preparation and properties of sulfonated or phosponated polybenzimidazoles and polybenzazoles, in E. Charles, Jr. Carraher, G.S. Graham (Eds.), Functional Condensation Polymers, Springer Science & Business Media, United State, 2007, pp. 101.

[30] L. L. Pluart, Epoxy-based nanocomposites, in: S. Thomas, G. Zaikov, Valsaraj, Meera (Eds.), Recent advances in polymer nanocomposite: synthesis and characterization, CRC Press, 2010, pp.75-136.

[31] A.H.M. Yusof, M.A.M. Amin, A.F. Ismail, M.N. Anam, A.N. Mahmud, Fabrication and effect of sulfonated poly (ether ether ketone) with Cloisite15A® nanoclays for microbial fuel cell application, Int. J. Sust. Construct. Eng. Tech. 4 (2013) 63-74.

[32] K.-V. Peinemann, S.P. Nunes, Membranes for energy conversion, Vol. 2, Wiley-VCH Verlag, GmbH & Co. KGaA, 2008.

[33] P. Choi, Investigation of thermodynamic and transport properties of proton-exchange membranes in fuel cell applications, Ph.D. Thesis, Worcester Polytechnic Institute, 2004.

[34] S.M.J. Zaidi, Preparation and characterization of composite membranes using blends of SPEEK/PBI with boron phosphate, Electrochim. Acta. 50 (2005) 4771–4777.